Available online at www.sciencedirect.com
ScienceDirect
Biochemical and Biophysical Research Communications 369 (2008) 225–239
BBRC
www.elsevier.com/locate/ybbrc

Infrared spectroscopic study of the metal-coordination structures of calcium-binding proteins

Masayuki Nara [a], Masaru Tanokura [b,*]

[a] Laboratory of Chemistry, College of Liberal Arts and Sciences, Tokyo Medical and Dental University, Chiba 272-0827, Japan
[b] Department of Applied Biological Chemistry, Graduate School of Agricultural and Life Sciences, University of Tokyo, 1-1-1 Yayoi, Bunkyo-ku, Tokyo 113-8657, Japan

Received 17 October 2007
Available online 7 January 2008

Abstract

Carboxylate (COO^-) groups can coordinate to metal ions in of the following four modes: 'unidentate', 'bidentate', 'bridging' and 'pseudo-bridging' modes. COO^- stretching frequencies provide information about the coordination modes of COO^- groups to metal ions. We review the Fourier-transform infrared spectroscopy (FTIR) of side-chain COO^- groups of Ca^{2+}-binding proteins: pike parvalbumin p*I* 4.10, bovine calmodulin and Akazara scallop troponin C. FTIR spectroscopy of Akazara scallop troponin C has demonstrated that the coordination structure of Mg^{2+} is distinctly different from that of Ca^{2+} in the Ca^{2+}-binding site. The assignments of the COO^- antisymmetric stretch have been ensured on the basis of the spectra of calcium-binding peptide analogues. The downshift of the COO^- antisymmetric stretching mode from 1565 cm^{-1} to 1555–1540 cm^{-1} upon Ca^{2+} binding is a commonly observed feature of FTIR spectra for EF-hand proteins.

Keywords: Infrared spectroscopy; Coordination structure; Carboxylate group; Parvalbumin; Calmodulin; Troponin C; Synthetic calcium-binding peptide

Calcium ion has a number of functions in biological systems, from biomineralisation in bones and teeth to a complex role as an intracellular messenger. The role of Ca^{2+} as an intracellular messenger has been recognised since the 1970s [1]. Kretsinger proposed that the actions of Ca^{2+} are the results of its binding to specific proteins considered to be Ca^{2+} receptors [2]. Like Ca^{2+}, Mg^{2+} is essential in biological systems, as it has both structural and catalytic functions [3]. Mg^{2+} is the most abundant divalent cation in mammalian cells, with a nearly constant cytosolic free concentration of 0.5–2.0 mM. The concentration of Ca^{2+} in the cytosol is 10^{-7} M, four orders of magnitude lower than that of Mg^{2+}. The cellular activities by Ca^{2+} are regulated through transient increases in the cytosolic concentration, from 10^{-7} M in a resting cell to 10^{-6}–10^{-5} M in an activated cell [4]. Thus, Ca^{2+} can regulate the functions of Ca^{2+}-binding proteins even in a 100- to 1000-fold excess of Mg^{2+}. Discrimination of the Ca^{2+}-binding protein against Mg^{2+} is achieved by taking advantage of the larger ionic radius of Ca^{2+} and, possibly, through a special arrangement of coordinating oxygen ligands: Ca^{2+} takes a coordination number of 6–8, less stringent than that of Mg^{2+}, which has a strong preference for six-fold coordination in an octahedral symmetry [5].

The Ca^{2+}-binding region is composed of about 30 amino-acid residues and has a conserved helix-loop-helix motif called the EF-hand domain [6,7]. The calcium-binding site involves a segment of a polypeptide chain having 12 continuous residues, which are arranged to coordinate Ca^{2+} with pentagonal bipyramid symmetry, with seven ligands provided by five side-chain oxygens of the carboxylate group etc., one backbone carbonyl oxygen and one water oxygen. Two of the side-chain ligands are provided by a highly conserved bidentate Glu in the 12th residue.

* Corresponding author. Fax: +81 3 5841 8023.
E-mail address: amtanok@mail.ecc.u-tokyo.ac.jp (M. Tanokura).

0006-291X/$ - see front matter © 2007 Elsevier Inc. All rights reserved.
doi:10.1016/j.bbrc.2007.11.188

Upon accommodation of Ca^{2+}, the EF-hand domain changes from a relatively compact, "closed" conformation to an "open" conformation, allowing the hydrophobic residues that had been hidden in the internal portions of Ca^{2+}-binding proteins to be exposed. The hydrophobic residues in the Ca^{2+}-binding proteins interact with their target proteins and control their activity in the cell.

The carboxylate (COO^-) groups can coordinate to metal ions in a number of modes (Fig. 1): 'unidentate' (or 'monodentate'), 'bidentate' (or 'chelating'), 'bridging' (or 'bridging bidentate'), and 'pseudo-bridging' modes [8,9]. When a metal ion interacts with only one oxygen atom of a COO^- group, the coordination structure is regarded as unidendate. In the bidentate coordination mode, the metal ion interacts equally with the two oxygen atoms of a COO^- group. In the bridging coordination mode, one metal ion binds to one of the two oxygens in a COO^- group and another metal ion to the other oxygen atom. As a special case of the bridging mode, the pseudo-bridging coordination mode features a water molecule replacing one of the two ligands in the bridging coordination. Extensive infrared studies have been done on the relationship between COO^- stretching frequencies and coordination types [8,10]. Deacon and Phillips [8] have found a general tendency in the relationship between $\Delta\nu_{a-s}$ (frequency separation between the COO^- antisymmetric and symmetric stretching vibrations) and the coordination types of the COO^- group to metal ions by examining the structures and vibrational frequencies of a number of acetate salts in the solid state. The frequency of the COO^- antisymmetric stretch of the unidentate species is higher than that of the ionic (metal-free) species, which is in turn higher than that of the bidentate species. The reverse is the case for the COO^- symmetric stretch. As a result, the $\Delta\nu_{a-s}$ values for unidentate, bridging, bidentate and ionic species are in the following order:

$$\Delta\nu_{a-s}(\text{unidentate}) > \Delta\nu_{a-s}(\text{ionic}) \sim \Delta\nu_{a-s}(\text{bridging}) > \Delta\nu_{a-s}(\text{bidentate}),$$

where $\Delta\nu_{a-s}$ (ionic) is approximately 160–170 cm^{-1}. *Ab initio* molecular orbital calculation revealed that the correlation is related to changes in the CO bond length and the OCO angle [11]. An equation for the relationship between the structure of the COO^- group and the value of $\Delta\nu_{a-s}$ (in cm^{-1}) is given as

$$\Delta\nu_{a-s} = 1818.1\delta r + 16.47(\theta_{OCO} - 120) + 66.8,$$

where δr is the difference between the two CO bond lengths (in Å) and θ_{OCO} is the OCO angle (in deg). This equation suggests that the variation of 0.01 Å in δr or 1° in θ_{OCO} gives rise to a change of 16–18 cm^{-1} in the value of $\Delta\nu_{a-s}$.

Fourier-transform infrared spectroscopy (FTIR) is a useful method for investigating protein structures in diverse environments [12–17]. The development of computerised Fourier-transform infrared instrumentation has not only improved the signal-to-noise ratio, but also made it possible to enhance the resolution of broad infrared bands by techniques such as Fourier self-deconvolution and second-derivative calculation [18–20]. Among the infrared bands created by the peptide group, the amide-I band has been the most widely used in studies of protein secondary structures. The amide-I mode consists mainly of the C═O stretch of the peptide group (mixed with the N—H bend and the C—N stretch) and gives rise to a strong infrared band in the region of 1700–1600 cm^{-1}. The relationship between the position of the amide-I band and the type of secondary structure has been investigated experimentally for model peptides and proteins of known three-dimensional structure [14]. The general empirical rule in the infrared study of proteins is to assign the individual amide-I bands resolved by resolution-enhancement techniques to representative secondary structures such as α-helix, β-sheet, β-turn and so on [21].

FTIR spectroscopy also has potential in the study of protein side chains such as aromatic rings —COO^-, —OH, —SH, —CH_3, —CH_2— and so on, to elucidate the mechanisms underlying protein reactions. Barth has reviewed the infrared absorption of amino-acid side chains in H_2O and D_2O [22]. As mentioned above, infrared spectroscopy provides information about the coordination modes of the COO^- groups of various acetate compounds in the solid state. The empirical rule described above can be applied to other compounds, such as amino acids (glutamic and aspartic) and ethylenediaminetetraacetic acid (EDTA), although the value $\Delta\nu_{a-s}$ (ionic) depends on the compound. When we apply this empirical rule to the side-chain COO^- groups contained in a protein in solution, we see that the COO^- group, which binds to M^{2+} (bicationic metal ion) in the unidentate coordination mode in the solid state, probably contacts water molecules in aqueous solution and may become a 'pseudo-bridging' coordination mode.

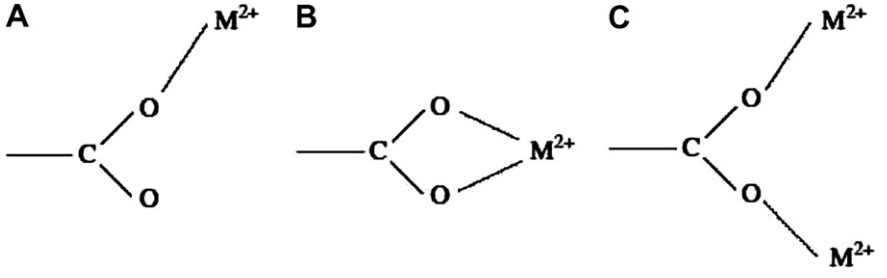

Fig. 1. Coordinating structures of the side-chain COO^- groups to M^{2+} in (A) unidentate, (B) bidentate, and (C) bridging modes.

This is applicable to [$EDTA^{4-}$–Ca^{2+}] complex in aqueous solution [23] and most of the side-chain COO^- groups in the unidentate coordination mode in Ca^{2+}-binding proteins, as mentioned below.

In this article we review the FTIR spectroscopy of side-chain COO^- groups of Ca^{2+}-binding proteins: pike parvalbumin p*I* 4.10 [24], bovine calmodulin (CaM) [25], Akazara scallop troponin C (TnC) [26–28] and calcium-binding peptide analogues [29]. First, we have presented FTIR studies on pike parvalbumin p*I* 4.10 [24] and CaM [25], where we have established that the COO^- stretches identify the coordination modes of COO^- groups on the level of Ca^{2+}-binding proteins. Second, we have shown the FTIR spectra of Akazara scallop TnC [26], a single Ca^{2+}-binding protein, and its site-directed mutants [27,28], where FTIR spectroscopy demonstrates that the coordination structure of Mg^{2+} is distinctly different from that of Ca^{2+} in the Ca^{2+}-binding site in solution. Finally, the assignments of the COO^- antisymmetric stretch were ensured on the basis of the spectra of calcium-binding peptide analogues [28,29].

Pike parvalbumin p*I* 4.10

Parvalbumins, which are ubiquitous in vertebrates, form a group in Ca^{2+}-binding proteins in parallel with calmodulin and troponin C [30]. Although the function of parvalbumins is not yet understood, their involvement in the relaxation process of fast muscles has been proposed [31,32]. Kretsinger and Nockolds [33] first reported the three-dimensional structure of carp parvalbumin (isoform p*I* 4.25) in crystal. According to their results, which Moew and Kretsinger later refined [34], this protein is globular and contains six helical parts called the A–F helices from the N-terminus, and has a feature common to Ca^{2+}-binding proteins, namely, the EF-hand motif, which is formed by about 30 amino-acid residues consisting of the E and F helices (nearly perpendicular to each other) and a connecting loop with a Ca^{2+}-binding site (EF site). Another domain of about 30 amino-acid residues containing the C and D helices also assumes a similar conformation with a Ca^{2+}-binding site in it (CD site).

An X-ray analysis of carp parvalbumin at 1.5 Å resolution by Kumar et al. [35] has shown that the Ca^{2+} ions in both the CD and EF sites are 7-coordinate; the ligands in the CD site are Asp-51, Asp-53, Ser-55 (O of the OH group), Phe-57 (O of the main chain CO group), Glu-59 and Glu-62; and those in the EF site are Asp-90, Asp-92, Asp-94, Lys-96 (O of the main chain CO group), Glu-101, and water-128. The COO^- groups of all of these aspartic acid residues and Glu-59 are unidentate, whereas those of Glu-62 and Glu-101 are bidentate.

The Mg^{2+} and Mn^{2+} ions have affinities for the Ca^{2+}-binding sites in parvalbumins, but the association constants for Mg^{2+} are three to four orders of magnitude smaller than those for Ca^{2+} [36,37]. Pike parvalbumin p*I* 4.10 is interesting for the purpose of studying the metal–ligand interactions in Ca^{2+}-binding proteins, because Declercq et al. [38,6] have reported the X-ray structures (1.6–1.8 Å resolution) of this protein for not only the Ca^{2+}-bound state but also the Mn^{2+}-bound state and a partially Mg^{2+}-bound state where the Mg^{2+} ion is bound only to the EF site. The primary structures of the two Ca^{2+}-binding sites in pike parvalbumin p*I* 4.10 are exactly the same as those of carp parvalbumin p*I* 4.25, and the X-ray structures of those two kinds of parvalbumins are essentially the same. In contrast to the Ca^{2+}-bound state, the COO^- groups of both Glu-62 and Glu-101 in the Mn^{2+}-bound state of pike parvalbumin are unidentate. The COO^- group of Glu-101 in the partially Mg^{2+}-bound form is also unidentate.

We have demonstrated that the comparison of the FTIR spectra of the metal-bound forms (metal = Mg^{2+}, Mn^{2+}, and Ca^{2+}) of pike parvalbumin p*I* 4.10 leads to unique identification of bands that can be used as markers for the types of coordination of the COO^- group to the metal ion in Ca^{2+}-binding proteins. Fig. 2 shows the infrared Fourier self-deconvolved and second-derivative spectra of the Mg^{2+}-bound, Mn^{2+}-bound and Ca^{2+}-bound states of deuterated pike parvalbumin p*I* 4.10. Significant differences were observed in the region of COO^- antisymmetric

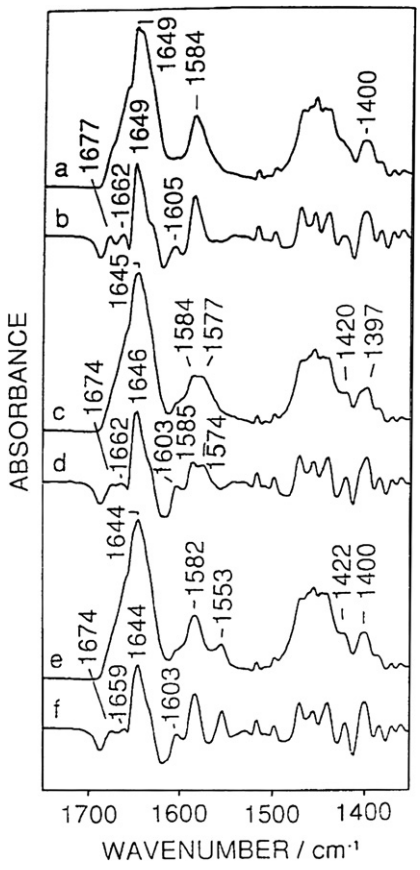

Fig. 2. Fourier self-deconvolved (a, c, and, e) and second-derivative (b, d, and f) spectra of (a and b) Mg^{2+}-bound, (c and d) Mn^{2+}-bound, and (e and f) Ca^{2+}-bound pike parvalbumin. Deconvolution was performed according to the method described by Jones and Shimokoshi [20]. Second derivatives are multiplied by −1. From Nara et al. [24].

stretch; there were two bands, at 1584 and 1577 cm^{-1}, in the Mn^{2+}-bound form, while there is a single band at 1584 cm^{-1} in Fig. 2a and b and at 1582 cm^{-1} in Fig. 2e and f. The band at 1553 cm^{-1} in Fig. 2e and f is characteristic of the Ca^{2+}-bound state.

The bands observed in the region of 1610–1550 cm^{-1} in Fig. 2 are correlated to the local environments of the COO^- groups in the protein molecule.

(a) The band at 1553 cm^{-1} of the Ca^{2+}-bound state is undoubtedly due to the COO^- groups of Glu-62 and Glu-101, which are coordinated to Ca^{2+} in the bidentate mode. The fact that this band is characteristic of the Ca^{2+}-bound form agrees completely with the results of X-ray analyses that the COO^- groups of Glu-62 and Glu-101 are bidentate only in the Ca^{2+}-bound form. The 1553 cm^{-1} band of the Ca^{2+}-bound form is 14 cm^{-1} downshifted from the 1567 cm^{-1} band of free glutamate. This downshift parallels that of the COO^- antisymmetric stretching band of the acetate anion ongoing from the 'ionic' state to the bidentate state.

(b) The band at 1577–1574 cm^{-1} in Fig. 2c and d is probably due to the COO^- groups of Glu-62 and Glu-101 in the Mn^{2+}-bound state, which are unidentate according to X-ray analysis [6]. This band is 7–10 cm^{-1} upshifted from the 1567 cm^{-1} band of 'free' glutamate in parallel with the upshift of the acetate ion ongoing from the 'ionic' state to the unidentate. These unidentate COO^- groups may change to the pseudo-bridging coordination mode in solution, since the upshifted value of 7–10 cm^{-1} is much smaller than those observed for acetate salts going from the 'ionic' to unidentate state.

(c) According to the X-ray analysis of the partially Mg^{2+}-bound form [6], the COO^- group of Glu-101 in this form is in the pseudo-bridging state. The band at 1584 cm^{-1} of the Mg^{2+}-bound state may contain a contribution from (COO^-) of Glu-101 in the pseudo-bridging mode, in addition to the absorption due to the 'free' COO^- groups of aspartate residues.

Calmodulin

Calmodulin regulates the functions of a wide variety of enzymes [31,32,39]. It has four Ca^{2+}-binding sites (I–IV). X-ray analyses [40,41] have revealed that these four sites are similar to the EF-hand motif reported on parvalbumin [33], and that the COO^- groups of Asp and Glu, the $CONH_2$ groups of Asn and so on are coordinated to Ca^{2+}. Bovine CaM has 17 Asp COO^- groups and 21 Glu COO^- groups in a molecule. Of these 38 COO^- groups, 16 exist in the Ca^{2+}-binding sites, and the COO^- groups of the following 14 amino-acid residues are directly coordinated to Ca^{2+}: Asp-20 (1), Asp-22 (3), Asp-24 (5), and Glu-31(12) in site I; Asp-56 (1), Asp-58 (3), and Glu-67 (12) in site II; Asp-93 (1), Asp-95 (3), and Glu-104 (12) in site III; and Asp-129 (1), Asp-131 (3), Asp-133 (5), and Glu-140 (12) in site IV, where the numbers in parentheses refer to the local sequential order of the amino-acid residues in each Ca^{2+}-binding site consisting of 12 residues. Studies on CaM obtained from various mutants have shown that the 12th Glu residues in sites I–IV (Glu-31, Glu-67, Glu-104, and Glu-140) are essential for Ca^{2+} binding [42], whereas the third Asp residue in site II (Asp-58) and that in site III (Asp-95) are associated with intersite cooperativity [43].

CaM binds various metal ions besides Ca^{2+} [44,45]. The correlation between CaM activities and the metal-ion radii has been studied by assaying CaM-dependent phosphodiesterase activity as well as tyrosine fluorescence [45]. FTIR and electron-spin-resonance spectroscopies and the assay of CaM-dependent myosin light-chain kinase activity have also been applied to the study of the interaction between CaM and various metal ions [46]. CaM's interaction with Mg^{2+} is interesting because CaM is thought to interact with not only Ca^{2+} but also Mg^{2+} under physiological conditions [47]. Comparative studies on the binding effects of Ca^{2+} and Mg^{2+} have been performed by using circular dichroism [48] and nuclear magnetic resonance [49] spectroscopies. Cd^{2+} is thought to be an effective substitute for Ca^{2+}, since the radii of these two cations are close to each other (1.00 Å for Ca^{2+} and 0.95 Å for Cd^{2+}).

FTIR studies on CaM have been reported by Trewhella et al. [50], Rainteau et al. [46] and Jackson et al. [51]. The amide-I′ bands of CaM in D_2O solution have been analysed by the method of Fourier self-deconvolution, second-derivative spectrum, and difference spectrum [50]. The metal-ion dependence of the half-width of the amide-II band has been reported on undeuterated CaM in nujol [46]. CaM's interactions with its peptides also have been studied by FTIR spectroscopy in combination with the isotope-edited method [52] or vibrational circular dichroism (VCD) spectroscopy [53].

We have utilised resolution-enhancement techniques to study the FTIR spectra of M^{2+}-bound CaM ($M^{2+} = Mg^{2+}$, Ca^{2+}, Sr^{2+}, and Cd^{2+}) as well as M^{2+}-free (apo) CaM in order to determine the correlations between the FTIR spectra and the function of CaM and to obtain information about structural changes induced by M^{2+} binding. By comparing the spectra of the Ca^{2+}-bound state with those of the M^{2+}-free state, we tried to find bands characteristic of active-type protein such as the Ca^{2+}-bound state and those of the inactive type such as the M^{2+}-free state. Fig. 3 shows infrared second-derivative spectra of the M^{2+}-bound and M^{2+}-free (apo) states of CaM. In the amide-I′ region, three bands were observed at 1674, 1660, and 1644 cm^{-1} in the spectrum of the Ca^{2+}-bound form [Fig. 3b], whereas only two bands were observed at 1675 and 1642 cm^{-1} in the spectrum of the M^{2+}-free state [Fig. 3e]. Since the 1660 cm^{-1} band of the Ca^{2+}-bound form is clearly observed, it is considered a band characteristic of the active type. Clear differences were found between the Ca^{2+}-bound and M^{2+}-free forms

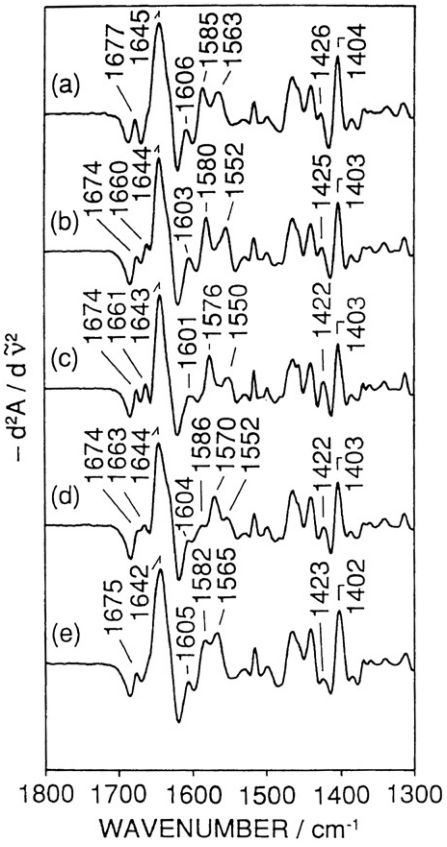

Fig. 3. FTIR second-derivative spectra of the M^{2+}-bound and M^{2+}-free (apo) states of calmodulin in D_2O solution: (a) Mg^{2+}-bound state; (b) Ca^{2+}-bound state; (c) Sr^{2+}-bound state; (d) Cd^{2+}-bound state; and (e) M^{2+}-free state. From Nara et al. [25].

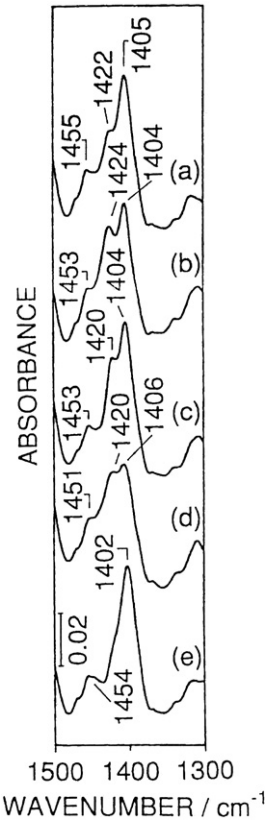

Fig. 4. FTIR spectra (1500–1300 cm^{-1}) of the M^{2+}-bound and M^{2+}-free states of calmodulin in H_2O solution. For (a)–(e), see the caption of Fig. 3. From Nara et al. [25].

in the region of COO^- antisymmetric stretch. The Ca^{2+}-bound state had two bands, at 1580 and 1552 cm^{-1}, in Fig. 3b and two at the M^{2+}-free state, at 1582 and 1565 cm^{-1}, in Fig. 3e. These spectra demonstrated that the 1552 cm^{-1} band is characteristic of the active type. In the COO^- symmetric stretching region, the intensity of the band at 1425 cm^{-1} of the Ca^{2+}-bound state in Fig. 3b seemed to be stronger than that of the corresponding band at 1423 cm^{-1} of the M^{2+}-free state in Fig. 3e. This difference is more clearly seen in the original spectra taken from H_2O solutions. The band at 1424 cm^{-1} of the Ca^{2+}-bound form apparently exists in Fig. 4b, whereas no definitive band is seen around this position in the spectrum of the M^{2+}-free form in Fig. 4e. Accordingly, the existence of a band at 1424 cm^{-1} in addition to a more intense band at about 1404 cm^{-1} may be regarded as a spectral feature of the active type. Consequently, the marker bands of the active form were: (1) the amide-I′ band at about 1661 cm^{-1}, (2) the COO^- antisymmetric stretching band at 1553 cm^{-1}, and (3) the COO^- symmetric stretching band at 1424 cm^{-1}. We call these bands markers I, II, and III, respectively.

The spectra of the Sr^{2+}- and Cd^{2+}-bound forms had similarities to those of the Ca^{2+}-bound form, whereas the spectrum of the Mg^{2+}-bound form was closer to that of the M^{2+}-free form. Marker I was seen in the second-derivative spectra of the Sr^{2+}- and Cd^{2+}-bound forms, whereas the Mg^{2+}-bound form did not show this marker band. Marker II was found at 1550 cm^{-1} for the Sr^{2+}-bound form and at 1552 cm^{-1} for the Cd^{2+}-bound form, but these bands are relatively weaker in intensity than the 1552 cm^{-1} band of the Ca^{2+}-bound form. Marker II was not clearly observed for the Mg^{2+}-bound form. Marker III was observed in the spectra of all the M^{2+}-bound forms, although the intensity of this marker band at 1424–1420 cm^{-1} relative to that of the band at 1406–1404 cm^{-1} varied with the metal ion. Marker band I is considered to be associated with a secondary structure of the protein main chain, and marker bands II and III with the interaction between M^{2+} and the COO^- groups in the side chains of Asp and Glu residues. The Mg^{2+}-bound form is definitely different from the Ca^{2+}-, Sr^{2+}-, and Cd^{2+}-bound forms, and is close to the M^{2+}-free form.

Chao et al. [47] have investigated the correlation between the radii of M^{2+} and the activities of the M^{2+}-bound form by measuring CaM-dependent phosphodiesterase activities. According to their results, the activities of the Mg^{2+}-, Sr^{2+}-, and Cd^{2+}-bound forms are 35%, 86%, and 90% of that of the Ca^{2+}-bound form, respectively. Since the ionic radii of Mg^{2+}, Ca^{2+}, Sr^{2+}, and Cd^{2+} are 0.72, 0.95, 1.00, and 1.16 Å, respectively, the

activity level of the M^{2+}-bound form tends to fall below that of the Ca^{2+}-bound form as the ionic radius of M^{2+} deviates from that of Ca^{2+}. There seems to be a broad parallel between the infrared intensities at about 1553 cm^{-1} (band II) and the order of activity levels of the M^{2+}-bound forms reported by Chao et al. [47]. The infrared intensities at about 1553 cm^{-1} seem to have the order $Ca^{2+} > Sr^{2+} > Cd^{2+} > Mg^{2+}$, although it is difficult to determine the intensities quantitatively because of the overlapping of closely located bands. The intensities at 1424–1420 cm^{-1} (band III) relative to that of 1406–1402 cm^{-1} in Fig. 4 also seemed to be associated with the activity level. The correlation between the intensities at 1663–1660 cm^{-1} in Fig. 3 and the M^{2+}-bound activities is not as obvious, because band I is not well resolved. In Fig. 3, however, band I is clearly observable only in the spectra of the Ca^{2+}-, Sr^{2+}-, and Cd^{2+}-bound states.

Akazara scallop troponin C

Muscle contraction of vertebrate skeletal and cardiac muscles is regulated by troponin in a Ca^{2+}-dependent manner [54]. Troponin contains three components: troponin C (TnC), troponin I and troponin T; TnC is the Ca^{2+}-binding component. In general, TnC contains two independent Ca^{2+}-binding domains, each consisting of two EF-hand motifs [55]. Vertebrate TnCs bind three or four Ca^{2+} ions in a molecule [56–58] and act as the Ca^{2+} switch of muscle contraction associated with the binding and release of one or two Ca^{2+} ions in the N-terminal domain. The N-terminal domain has thus been called the regulatory domain and contains one or two low-affinity Ca^{2+}-binding sites [59]. On the other hand, the C-terminal domain has been called the structural domain and contains two high-affinity sites. They also bind Mg^{2+} and are called Ca^{2+}/Mg^{2+} sites. Although the N-terminal low-affinity sites are called Ca^{2+}-specific sites, they also bind Mg^{2+} very weakly [60,61]. Since the intracellular Mg^{2+} concentration is relatively high at about 1 mM [62,63], intracellular Mg^{2+} ions are bound to the low-affinity Ca^{2+}-binding sites in addition to high-affinity sites in resting muscle cells [61]. It is therefore important to know the structural differences between the Ca^{2+}- and Mg^{2+}-bound forms.

Invertebrate muscles also have troponin molecules, and their TnCs bind less Ca^{2+} than do vertebrate ones, because they have lost the Ca^{2+}-binding ability at several sites due to the replacement of amino acids critical to chelate Ca^{2+} [64]. Akazara scallop is an invertebrate. Its striated adductor muscle contains TnC that works as a Ca^{2+} switch of contraction [65], and it binds only one Ca^{2+} ion at the C-terminal EF-hand motif [66]. Akazara scallop TnC is thus a curious and interesting molecule, since it regulates muscle contraction by binding a single Ca^{2+} ion.

Our interest is focused on the coordination structures of Mg^{2+} and Ca^{2+} in the Ca^{2+}-binding site as well as the protein conformation. The Ca^{2+}-binding loop (site IV) of this protein is composed of DTDGSGTVDYEE (residues 131–142) [66]. Applying the general rule of the EF-hand motif [33] to this protein, the COO^- groups of Asp-131, Asp-133 and Glu-142 should coordinate to Ca^{2+} directly. On the basis of the crystal structure of vertebrate TnCs [67,68], the COO^- group of Glu at the 12th position in site IV may coordinate to the Ca^{2+} ion in the bidentate mode and to the COO^- groups of Asp at the 1st and 3rd positions in the unidentate mode.

Wild-type

We have measured FTIR spectra of Akazara scallop TnC to clarify the interaction of the side-chain COO^- groups with Ca^{2+} and Mg^{2+} ions in the Ca^{2+}-binding site. Fig. 5 shows the infrared second-derivative spectra of apo, Mg^{2+}-bound and Ca^{2+}-bound Akazara scallop TnC in D_2O across the range of 1750–1350 cm^{-1}. The patterns of the amide-I′ region (1700–1620 cm^{-1}) and the COO^- stretching region (1430–1370 cm^{-1}) were similar to one another; the bands at 1674, 1646, and 1402–1 cm^{-1} were observed in each state. Significant differences were observed in the region of the COO^- antisymmetric stretch (1620–1530 cm^{-1}). In the apo state (Fig. 5a), two

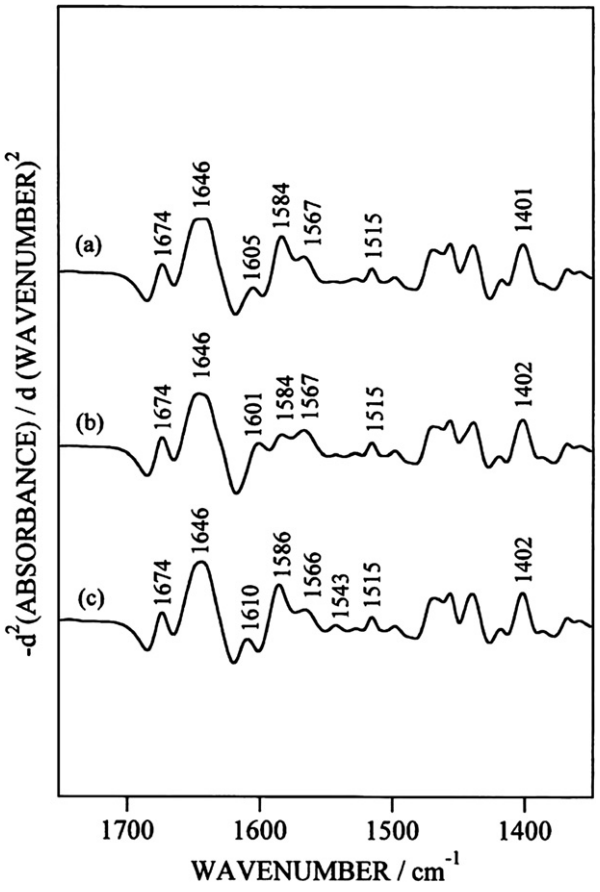

Fig. 5. FTIR second-derivative spectra of (a) M^{2+}-free, (b) Mg^{2+}-bound and (c) Ca^{2+}-bound Akazara scallop troponin C in solutions containing 40 mM Hepes–NaOD (pD 7.4) and 100 mM KCl. From Yumoto et al. [26].

strong bands were observed, at 1584 and 1567 cm^{-1}, that were due to the side-chain COO^- groups of Asp and Glu, respectively. Bands were also observed at 1601 cm^{-1} in the Mg^{2+}-bound state (Fig. 5b) and at 1543 cm^{-1} in the Ca^{2+}-bound state (Fig. 5c). The intensity of the 1567-cm^{-1} band in the Mg^{2+}-bound state was stronger than that in the Ca^{2+}-bound one, but identical to that in the apo one. The intensity of the 1584-cm^{-1} band in the Mg^{2+}-bound state was obviously smaller than that in the apo state, whereas the corresponding band in the Ca^{2+}-bound state showed a band at 1586 cm^{-1}, slightly higher in wavenumber than that in the apo state. The weak bands at 1605 cm^{-1} for the apo state and 1610 cm^{-1} for the Ca^{2+}-bound state may also be due to side-chain COO^- groups.

Fig. 6 shows the 1750–1350 cm^{-1} region of the difference spectra between the M^{2+}-bound and apo states. Fig. 6 provides additional significant information on the COO^- antisymmetric stretching region; the negative band at 1581 cm^{-1} in Fig. 6a, and both the positive one at 1592 cm^{-1} and the negative one at 1573 cm^{-1} in Fig. 6b. In the amide-I′ region, the intensity of 1646 cm^{-1} increased slightly upon Ca^{2+} binding, whereas no such change was observed upon Mg^{2+} binding. In addition, it should be noted that an upshift of the COO^- symmetric stretching band from 1396 to 1428–1425 cm^{-1} occurred upon Mg^{2+} or Ca^{2+} binding.

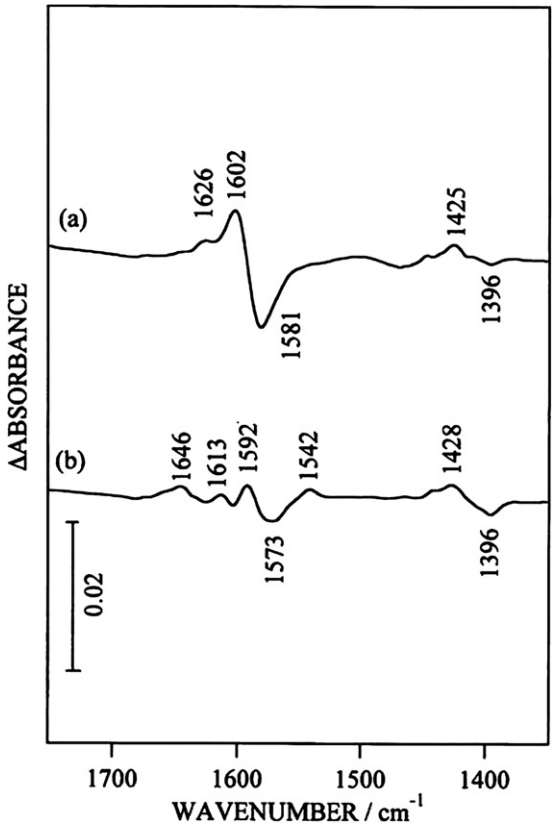

Fig. 6. FTIR difference spectra of Akazara scallop troponin C induced by (a) Mg^{2+} binding and (b) Ca^{2+} binding. From Yumoto et al. [26].

We have interpreted the bands in the COO^- antisymmetric stretching region for Akazara scallop TnC in relation to the coordination structures of the COO^- group and the peak positions of COO^- stretching bands mentioned above. (1) The 1543-cm^{-1} band in Fig. 5c is due to side-chain Glu-142 COO^- coordinated to the Ca^{2+} ion in the bidentate mode. This band was not observed in the Mg^{2+}-bound state, and the intensity at 1567 cm^{-1} in the Mg^{2+}-bound state was the same as that in the apo state. Therefore, this COO^- group does not coordinate Mg^{2+} directly. (2) The bands at 1602 cm^{-1} for the Mg^{2+}-bound state in Fig. 6a and at 1592 cm^{-1} for the Ca^{2+}-bound state in Fig. 6b indicate that the COO^- groups of Asp-131 and Asp-133 interact with Ca^{2+} as well as Mg^{2+} in the pseudo-bridging mode. This is direct evidence that Akazara scallop TnC interacts with Mg^{2+} in the single Ca^{2+}-binding site. (3) The shift of the COO^- symmetric stretch from 1396 to 1425 cm^{-1} in Fig. 6a also reflects that the COO^- groups interact with Mg^{2+} in the pseudo-bridging mode, because the peak positions for the COO^- symmetric and antisymmetric stretching vibrations move together. In addition, the weak band at 1605 cm^{-1} for the apo state and at 1610 cm^{-1} for the Ca^{2+}-bound state may be due to side-chain COO^- groups.

The effects of Mg^{2+} and Ca^{2+} binding in Akazara scallop TnC were also investigated by CD spectroscopy. The α-helix contents for apo, Mg^{2+}-bound, and Ca^{2+}-bound TnC were estimated as 36%, 41%, and 39%, respectively, according to the method reported by Provencher et al. [69]. As a result, most of the secondary structures were conserved among them. Therefore, most of the secondary structures of Akazara scallop TnC may not be affected upon either Mg^{2+} or Ca^{2+} binding. The effects of Mg^{2+} or Ca^{2+} binding on Akazara scallop TnC were also examined by gel-filtration chromatography and fluorescence spectroscopy. As a result, the sizes of TnC molecules had the following order: apo TnC > Mg^{2+}-bound TnC > Ca^{2+}-bound TnC. The fluorescence spectra across the range of 290–450 nm showed that the intensities at 350 nm had the following order: Ca^{2+}-bound TnC > Mg^{2+}-bound TnC ∼ apo TnC. Consequently, the tertiary structure of Ca^{2+}-bound TnC was slightly different from that of the Mg^{2+}-bound one as well as that of the apo state.

On the basis of the present results, we propose a model for the on–off mechanism in the activation of Akazara scallop TnC (Fig. 7). The Mg^{2+}-bound and Ca^{2+}-bound states may be regarded, respectively, as the resting and activated ones for muscle contraction, although the apo state may be the resting one under physiological conditions. First, in the Mg^{2+}-bound state, Asp-131 and Asp-133 interact with the Mg^{2+} ion in the pseudo-bridging mode, whereas Glu-142 does not interact with the Mg^{2+} ion. Asp-139 may be a ligand for the Mg^{2+} ion. Next, when Mg^{2+} is replaced by Ca^{2+} in the binding site by the stimulation, Glu-142 interacts with the Ca^{2+} ion in the bidentate mode, whereas Asp-131 and Asp-133 interact with the Ca^{2+} ion in the pseudo-bridging mode. The Ca^{2+} affinity is higher than

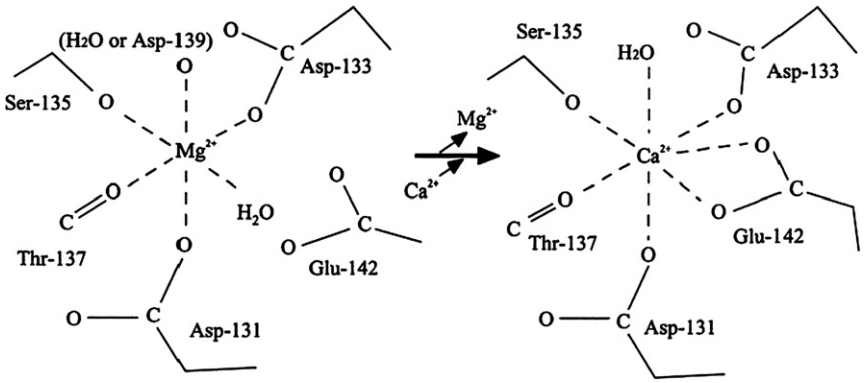

Fig. 7. A schematic model of changes in coordination structure of the Ca^{2+}-binding site of Akazara scallop troponin C accompanying the exchange of Mg^{2+} with Ca^{2+}. From Yumoto et al. [26].

the Mg^{2+} affinity, because Mg^{2+} has been easily replaced by Ca^{2+} but Ca^{2+} has not been easily replaced by Mg^{2+}. The Glu-142 COO^- group plays a critical role in the selectivity between Ca^{2+} and Mg^{2+} for the Ca^{2+}-binding site and may be critical for the affinity for Ca^{2+}. Thus, it has been recognised that the side-chain COO^- groups in the Ca^{2+}-binding site are important for the interaction of EF-hand proteins with divalent metal ions and the selectivity between Mg^{2+} and Ca^{2+}. Our result about the Mg^{2+} ligation of Akazara scallop TnC is close to the model proposed by Malmendal et al. [70]; Mg^{2+} binding occurs without ligation of the side-chain COO^- of Glu at the 12th position in the Ca^{2+}-binding loops of CaM.

Site-directed mutants of Akazara scallop TnC (E142Q and E142D)

FTIR spectroscopy was applied to study the coordination structure of Mg^{2+} in a site-directed mutant (E142Q) of Akazara scallop TnC. For simplicity, this mutant is called E142Q in this manuscript. Fig. 8 shows the infrared second-derivative spectra of apo and Mg^{2+}-bound E142Q in D_2O across the range of 1710–1500 cm^{-1}. The spectral patterns of the amide-I′ region were similar to each other, and therefore the overall main-chain conformation is thought to be conserved upon Mg^{2+} binding. On the other hand, the spectral patterns of the COO^- antisymmetric

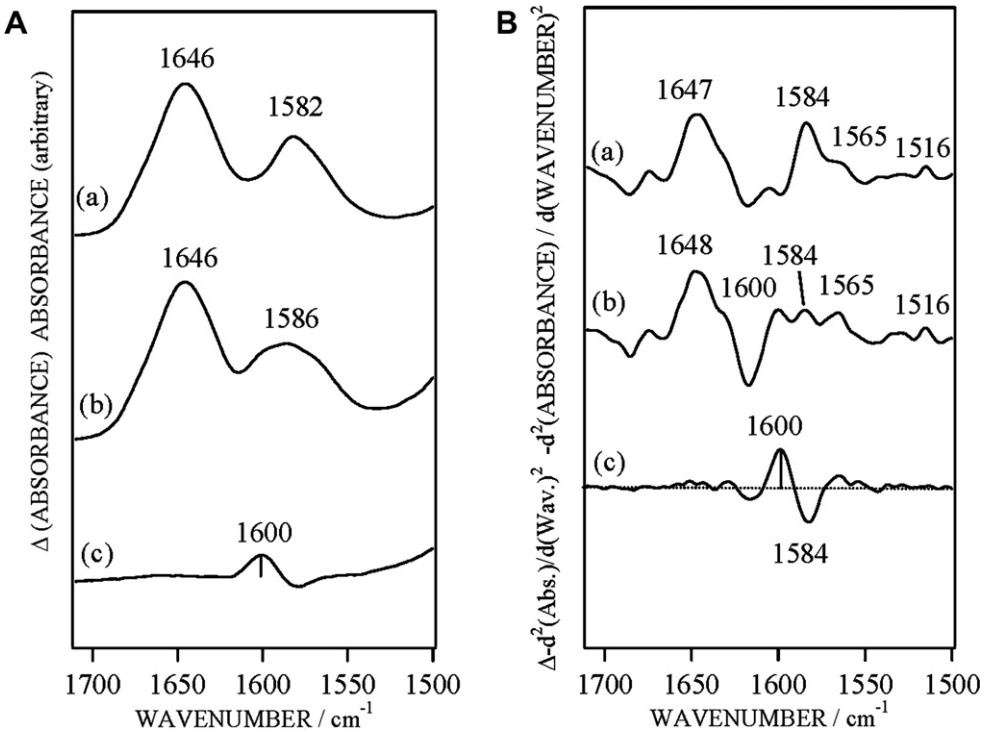

Fig. 8. FTIR absorption (A) and second-derivative (B) spectra of (a) apo and (b) Mg^{2+}-bound E142Q mutant. For each absorption and second-derivative spectra, the difference spectrum (c) was obtained by subtracting spectrum (a) from spectrum (b). Second derivatives are multiplied by −1. From Nara et al. [27].

stretching region were different among them. The band at 1584 cm^{-1} and a shoulder at 1565 cm^{-1} in the apo state (Fig. 8a) were, respectively, assigned to the β-COO^- group of Asp and the γ-COO^- group of Glu. The partial upshift of the 1584-cm^{-1} band to 1600 cm^{-1} upon Mg^{2+} binding (Fig. 8b) was due to the pseudo-bridging coordination of COO^- groups of Asp-131 and Asp-133, on the basis of the results for the wild-type. On account of the replacement of Glu to Gln, the band at 1565 cm^{-1} seemed to be slightly weaker than that of the wild-type. It should be noted that no significant downshift of the COO^- antisymmetric stretching band was observed upon Ca^{2+} binding (data not shown), since E142Q does not provide a bidentate coordination of the COO^- group at the 12th position of site IV.

We examined Mg^{2+} titration experiments for E142Q as well as for the wild-type of Akazara scallop TnC by monitoring the band at 1600 cm^{-1}. The intensity changes at 1600 cm^{-1} were evaluated by the amplitude difference between the second derivatives, as shown in Fig. 8c. Titration plots for E142Q and the wild-type are shown in Fig. 9. The results indicated that their binding constants for Mg^{2+} have the same value as each other (about 6 mM). Consequently, these experiments demonstrated that the side-chain COO^- group of Glu-142 has no relation to the Mg^{2+}-ligation.

The effects of Mg^{2+} and Ca^{2+} binding on E142Q were investigated by CD spectroscopy. The CD spectrum in each state showed two negative peaks, at 208 and 222 nm. Little change occurred upon Mg^{2+} or Ca^{2+} binding. Therefore, most of the secondary structures were conserved among them, consistent with the similarity in the patterns of the amide-I region in Fig. 8. The effects of Mg^{2+} or Ca^{2+} binding on Akazara scallop TnC were also examined by fluorescence spectroscopy. The fluorescence spectra across the range of 290–450 nm showed almost the same intensities at 350 nm. Consequently, the tertiary structure of Mg^{2+}-bound Akazara scallop TnC was identical to that of the Ca^{2+}-bound one as well as to that of the apo one.

These results indicate that Mg^{2+} binding to Akazara scallop TnC is of physiological relevance, because the binding constant of Akazara scallop TnC for Mg^{2+} was about 6 mM. Since intracellular Mg^{2+} concentration is relatively high at about 1 mM [62,63], the intracellular Mg^{2+} ion may bind Akazara scallop TnC in the resting muscle cells, although its single Ca^{2+}-binding site is apparently Ca^{2+}-specific [71]. Because the affinity of E142Q for Mg^{2+} was almost the same as that of the wild-type, the side-chain COO^- group of Glu-142 has no relation to the Mg^{2+}-ligation. Like the wild-type, the Mg^{2+} binding to E142Q had little effect on secondary and tertiary structures. On the other hand, the Ca^{2+} binding to E142Q has little effect on the secondary or tertiary structures, whereas the Ca^{2+} binding to the wild-type causes both secondary and tertiary structural changes. Therefore, the bidentate coordination of the Glu-142 COO^- group for Ca^{2+} is the trigger for the activation of Akazara scallop TnC, whereas the

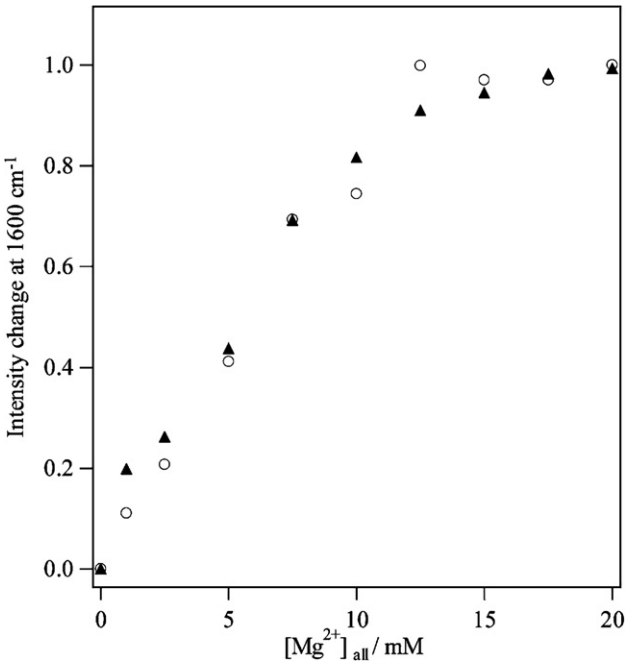

Fig. 9. Mg^{2+} titration plots of the E142Q mutant (▲) and wild-type (○) of Akazara scallop TnC. The band at 1600 cm^{-1}, which is due to the side-chain COO^- groups of Asp-131 and Asp-133 binding to Mg^{2+} in the pseudo-bridging coordination, was used for the marker of Mg^{2+}-ligation. Relative change was obtained by subtracting the spectrum of the apo state from that in each total Mg^{2+} concentration ($[Mg^{2+}]_{Total}$). The value of the vertical axis was scaled as the difference between the apo state and the $[Mg^{2+}]_{Total} = 20$ mM state becomes 1. From Nara et al. [27].

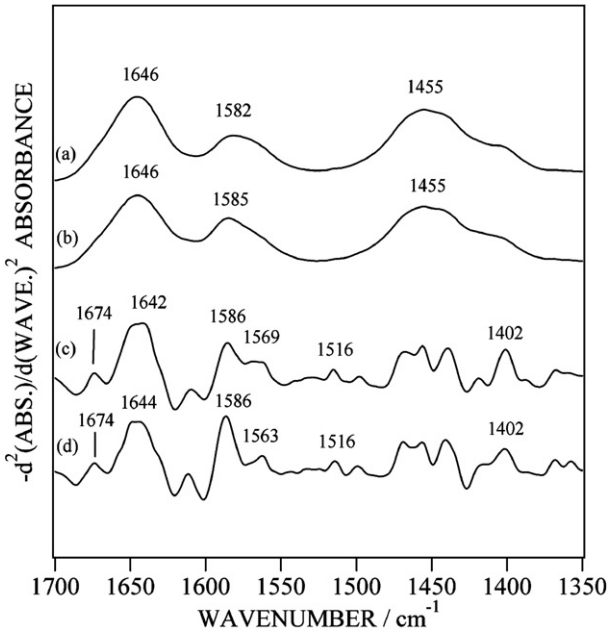

Fig. 10. Infrared absorption spectra of Ca^{2+}-bound (a) E142D and (b) E142Q mutants and second-derivative spectra of Ca^{2+}-bound (c) E142D and (d) E142Q mutants of Akazara scallop TnC in D_2O solution. Second derivatives are multiplied by −1. From Nara et al. [28].

pseudo-bridging coordinations of the Asp-131 and -133 COO^- groups do not serve as the trigger directly.

FTIR spectroscopy was also applied to study the coordination structure of Ca^{2+} bound in the site-directed mutant of Akazara scallop TnC, where Glu-142 is replaced by aspartic acid. We refer to this as the "E142D" mutant. The E142D mutant is interesting because Asp-142 has the potential to act as a chelate for Ca^{2+}. Fig. 10 shows the infrared absorption and second-derivative spectra of Ca^{2+}-bound E142D and E142Q of Akazara scallop TnC across the range of 1700–1350 cm^{-1}. It was difficult to distinguish them by the absorption spectra in Fig. 10a and b. The second-derivative calculation provides more detailed information about the spectral differences. As shown in Fig. 10c and d, there was no band around 1543 cm^{-1} for either the E142Q mutant or the E142D mutant, although the wild-type showed a band at about 1543 cm^{-1} in the Ca^{2+}-bound state. This result is consistent with our former conclusion that the 1543 cm^{-1} band is due to the Glu-142 side-chain COO^- group binding to Ca^{2+} in the bidentate coordination mode. The E142D mutant has a COO^- group at the 12th position of the calcium-binding site, but a downshift of the COO^- antisymmetric stretching mode was not observed upon Ca^{2+} loading, indicating that this group does not bind with Ca^{2+} in the bidentate coordination mode.

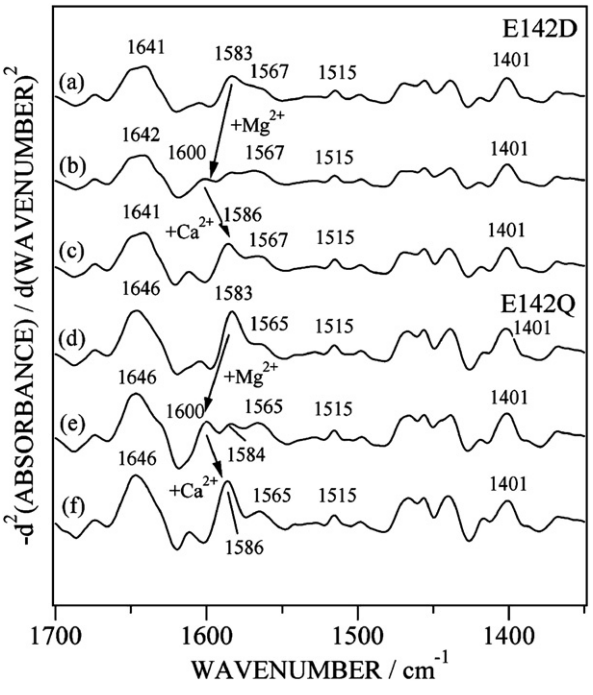

Fig. 11. Infrared second-derivative spectra of (a) apo E142D, (b) Mg^{2+}-loaded E142D, (c) Mg^{2+}/Ca^{2+} loaded E142D, (d) apo E142Q, (e) Mg^{2+}-loaded E142Q, and (f) Mg^{2+}/Ca^{2+} loaded E142Q mutants. Sample solutions were [TnC] = 2 mM and [KCl] = 100 mM for the apo state, [TnC] = 2 mM, [Mg^{2+}] = 20 mM, and [KCl] = 100 mM for the Mg^{2+}-loaded state; and [TnC] = 2 mM, [Mg^{2+}] = 20 mM, [Ca^{2+}] = 20 mM, and [KCl] = 100 mM for the Mg^{2+}-loaded state. From Nara et al. [28].

Fig. 11 shows the infrared second-derivative spectra of apo, Mg^{2+}-loaded and Mg^{2+}/Ca^{2+}-loaded E142D and E142Q mutants across the range of 1700–1350 cm^{-1}. At a glance, the spectral patterns of apo E142D (Fig. 11a) and apo E142Q (Fig. 11d) were, respectively, similar to those of Ca^{2+}-loaded E142D (Fig. 10c) and Ca^{2+}-loaded E142Q (Fig. 10d), since the "Ca^{2+}-binding marker" around 1543 cm^{-1} was not available for these mutants. The spectral patterns of the amide-I′ region were similar to one another, and therefore the overall main-chain conformation is thought to be conserved upon Mg^{2+} and/or Ca^{2+} loading. As shown in Fig. 11b, the Mg^{2+}-loaded E142D exhibited the characteristic band around 1600 cm^{-1}, which is due to Asp-131 and Asp-133 binding to Mg^{2+} in the pseudo-bridging coordination mode. The spectral pattern for Mg^{2+}/Ca^{2+}-loaded E142D is the same as that of the Ca^{2+}-loaded one (Fig. 10c), meaning that Mg^{2+} was completely replaced by Ca^{2+} in site IV. Therefore, it is concluded that the Mg^{2+}–Ca^{2+} exchange occurred for the E142D mutant like it did for the wild-type protein. Needless to say, the Mg^{2+}–Ca^{2+} exchange also occurred for the E142Q mutant (Fig. 11d–f). The intensity of the band at 1588 cm^{-1} seemed stronger for the Ca^{2+}-bound form than for the apo form, indicating that Asp-131 and Asp-133 bind to Ca^{2+} in the pseudo-bridging coordination mode. The bands at 1600 cm^{-1} for the E142D and E142Q mutants decreased accompanying the exchange of Mg^{2+} with Ca^{2+}. This strongly supported that the Mg^{2+}–Ca^{2+} exchange occurs in site IV only, and that therefore Mg^{2+} does not bind to the other sites.

Synthetic peptide analogues of Ca^{2+}-binding site: site IV of Akazara scallop TnC and site III of rabbit skeletal muscle TnC

The use of the synthetic calcium-binding peptide approach has provided valuable results for understanding the calcium-binding properties thus far [72–75]. Calcium binding to a series of peptides derived from site III of rabbit skeletal muscle TnC has been studied by Reid et al. [72], who found that a 34-residue peptide was required for relatively tight calcium binding. Shorter peptides have decreased calcium affinity, and the isolated 12-residue Ca^{2+}-binding loop binds to Ca^{2+} very weakly [73]. Thus, the length of the peptide is important for Ca^{2+} binding.

Site IV of Akazara scallop TnC

Fig. 12 shows the infrared second-derivative spectra for synthetic 17-residue peptide analogues for site IV of Akazara scallop TnC (wild-type) [Ac-DTDGSGTVDYEEFKBLM-NH_2] and for site-directed mutated ones (E142D, E142Q, and E142A) in the apo- and Ca^{2+}-loaded states. We chose a 17-residue peptide as the model Ca^{2+}-binding peptide, which corresponds to a calcium-binding site with the following five amino-acid residues. It also corresponds to the rabbit skeletal muscle TnC fragment, which is the minimum peptide

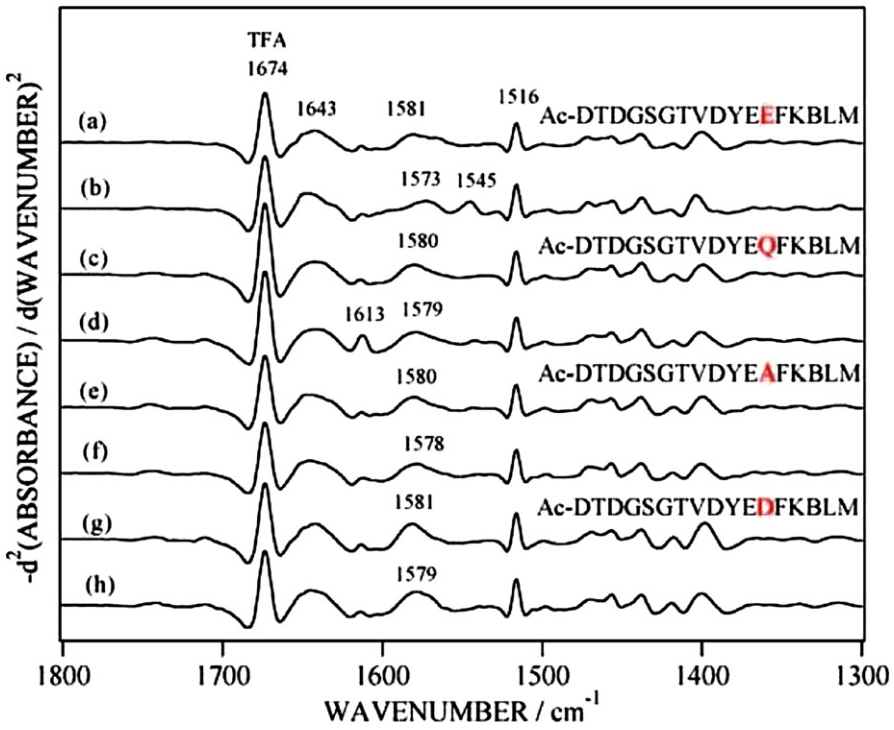

Fig. 12. Infrared second-derivative spectra for synthetic 17-residue peptide analogues for site IV of Akazara scallop TnC (wild-type) in (a) the apo- and (b) the Ca^{2+}-loaded states, E142D mutant in (c) the apo- and (d) the Ca^{2+}-loaded states, E142Q mutant in (e) the apo- and (f) the Ca^{2+}-loaded states and E142A mutant in (g) the apo- and (h) the Ca^{2+}-loaded states in D_2O solution. The amino-acid sequences are Ac-DTDGSGTVDYEEFKBLM-NH_2 for the wild-type, Ac-DTDGSGTVDYEDFKBLM-NH_2 for the E142D mutant, Ac-DTDGSGTVDYEQFKBLM-NH_2 for the E142Q mutant and Ac-DTDGSGTVDYEAFKBLM-NH_2 for the E142A mutant. The band at 1674 cm^{-1} is mainly due to trifluoroacetate (TFA), which is thought to be introduced during purification. From Nara et al. [28].

necessary for the interaction between the side-chain COO^- of Glu at the 12th position and Ca^{2+} in the bidentate coordination mode, as described in 'site III of rabbit skeletal muscle Tnc'. The peptide analogue for the wild-type showed a band at 1545 cm^{-1} in the Ca^{2+}-loaded state, which was not observed in the apo state. This band is almost consistent with that at 1543 cm^{-1} for Ca^{2+}-bound wild-type Akazara scallop TnC. Therefore, the band at 1543 cm^{-1} is undoubtedly assigned to the Glu-142 side-chain COO^- binding to Ca^{2+} in the bidentate coordination mode. The peptide analogues for site-directed mutants such as E142D, E142Q, and E142A showed no band around 1545 cm^{-1} even in the Ca^{2+}-loaded state. These results are consistent with those of the E142D and E142Q mutants of Akazara scallop TnC. Consequently, it was confirmed that the assignment of 1543 cm^{-1} for Ca^{2+}-bound Akazara scallop TnC described above using the synthetic peptide analogue approach is correct.

The physiological activity of Akazara scallop TnC has been reported only in the wild-type and E142Q forms [76]. The Ca^{2+}-loaded E142Q mutant is inactive due to the replacement of E with Q at the 12th position of site IV. The E142D mutant also may be inactive in the Ca^{2+}-loaded state, because the side-chain COO^- group at the 12th position does not serve as the ligand for Ca^{2+} directly. To elucidate the function of Akazara scallop TnC, it will be necessary to investigate not only TnC alone but also the troponin complex.

Site III of rabbit skeletal muscle TnC

We examined a series of synthetic peptide analogues for rabbit skeletal muscle TnC site III (Fig. 13) to understand the relationship between the amino-acid length of the synthetic peptide and the formation of the Ca^{2+} coordination structure. Fig. 14 shows the second-derivative spectra of (a) Mg^{2+}-loaded and (b) Ca^{2+}-loaded peptide I (corresponding to an EF-hand motif) [72,74], (c) Mg^{2+}-loaded and (d) Ca^{2+}-loaded peptide II (corresponding to a calcium-binding site) [73] in D_2O across the range of 1800–1300 cm^{-1}. Comparing the Mg^{2+}-loaded peptide I with the Ca^{2+}-loaded one, the patterns of the amide-I′ region were similar to each other; the bands at 1674 and 1640 cm^{-1} were observed in each state (Fig. 14a and b). Significant differences were observed in the region of COO^- antisymmetric stretching vibration (1610–1530 cm^{-1}); three bands were observed, at 1609, 1583, and 1563 cm^{-1}, in the Mg^{2+}-loaded state (Fig. 14a), while four bands were observed, at 1607, 1581, 1565, and 1552 cm^{-1}, in the Ca^{2+}-loaded state (Fig. 14b). The bands at 1583–1581 and 1564 cm^{-1} observed for both states are mainly due to uncoordinated (free) Asp and Glu side-chain COO^- groups, respectively. The band at 1552 cm^{-1} for Ca^{2+}-loaded peptide I is assigned to the side-chain COO^- group of Glu at the 12th position serving as the ligand for Ca^{2+} in the bidentate coordination mode. Based on the analogy to the FTIR studies on Akazara scallop TnC

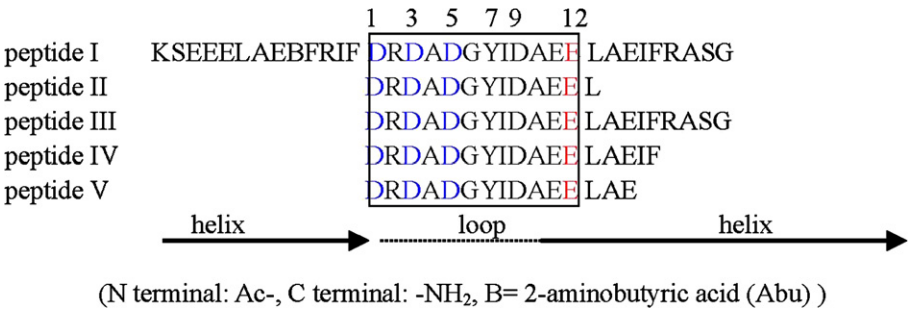

Fig. 13. Amino-acid sequences of synthetic peptide analogues of the Ca^{2+}-binding site III from rabbit skeletal muscle TnC. From Nara et al. [29].

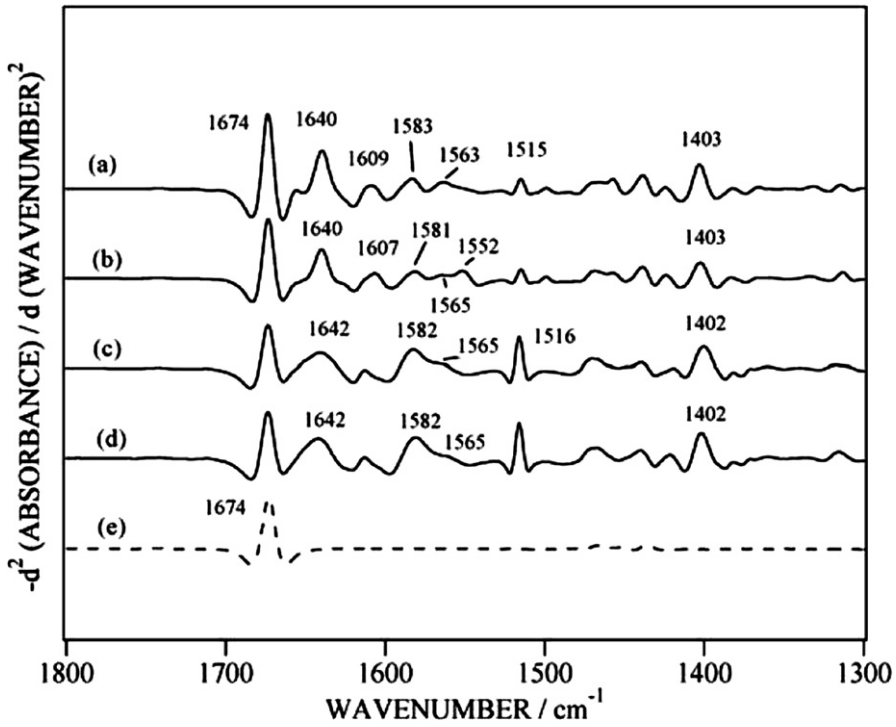

Fig. 14. Infrared second-derivative spectra of (a) Mg^{2+}-loaded and (b) Ca^{2+}-loaded peptide I (corresponding to an EF-hand motif), (c) Mg^{2+}-loaded and (d) Ca^{2+}-loaded peptide II (corresponding to a calcium-binding site with the following Leu-) in D_2O solution. Dotted line shows the second-derivative spectra of trifluoroacetate (TFA). Second derivatives are multiplied by −1. From Nara et al. [29].

described above, the band at 1609 cm^{-1} in the Mg^{2+}-loaded state and that at 1607-cm^{-1} in the Ca^{2+}-loaded state may be due to the side-chain COO^- group of Asp at the 1st, 3rd, and 5th positions serving as the ligand for M^{2+} in the pseudo-bridging coordination mode. On the other hand, there was no difference between the Mg^{2+}-loaded peptide II and the Ca^{2+}-loaded one even in the second-derivative spectra. These spectral patterns in Fig. 14c and d were the same as that of apo peptide II (data not shown). Therefore, it was concluded that peptide II has little or no affinity for Ca^{2+} or for Mg^{2+}.

Fig. 15 shows the infrared second-derivative spectra (1800–1300 cm^{-1}) for Mg^{2+}-loaded and Ca^{2+}-loaded peptides III–V. The spectral pattern for each peptide in the Mg^{2+}-loaded state was the same as that for the corresponding peptide in the apo state (data not shown), meaning that shorter peptides (III–V) have no affinity for Mg^{2+}. Peptides III and IV exhibited bands at 1555 and 1554 cm^{-1}, respectively, while peptide V did not exhibit a corresponding band. The band at about 1552 cm^{-1} is the Ca^{2+}-binding marker band, because this reflects the formation of the Ca^{2+}-bound coordination structure. Therefore, peptides III and IV bind to Ca^{2+}, but peptide V does not bind to Ca^{2+} directly under the condition of $[Ca^{2+}]/[peptide] = 10$. We found that, like peptide I, a loop-helix peptide (peptide III) can bind to Ca^{2+} even if it lacks an N-terminal-side helix.

We investigated the relationship between the amino-acid length of synthetic peptide analogues and the formation of Ca^{2+}-bound coordination structure. We found that the 17-residue peptide (peptide IV) seems to be the minimum Ca^{2+}-binding peptide necessary for the interaction between the side-chain COO^- of Glu at the 12th position and Ca^{2+} in the bidentate coordination mode. Our results suggest

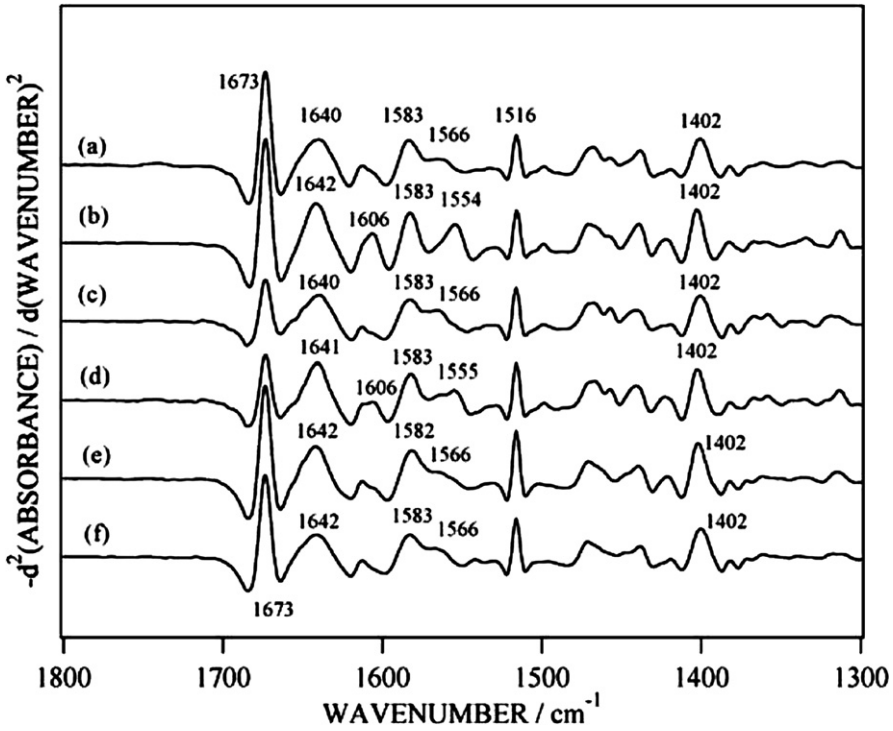

Fig. 15. Infrared second-derivative spectra of (a) Mg^{2+}-loaded and (b) Ca^{2+}-loaded peptide III (21-residue corresponding to loop-helix), (c) Mg^{2+}-loaded and (d) Ca^{2+}-loaded peptide IV (17-peptide), (e) Mg^{2+}-loaded and (f) Ca^{2+}-loaded peptide V (15-peptide) in D_2O solution. Second derivatives are multiplied by −1. From Nara et al. [29].

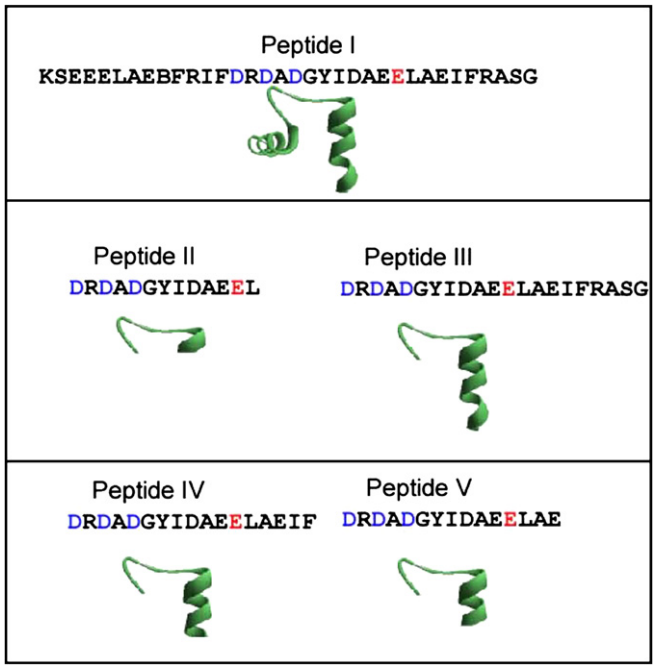

Fig. 16. Ribbon diagram of peptides I–V on the basis of the crystal structure (PDB: 2TN4). From Nara et al. [29].

that the C-terminal-side helix conformation is important for the contribution of the Glu side-chain COO^- group at the 12th position as the ligand. Peptide IV contains eight residues out of the C-terminal-side helix (12 residues: AEELAEIFRASG), but peptide V contains only six residues. As shown in Fig. 16, we visualised the structures of peptides I–V by using WebLab Viewer Lite (Accelys, San Diego) on the basis of the PDB data (2TN4) of rabbit fast skeletal troponin C [77]. The ribbon diagrams suggest that peptide V has less than two turns of the C-terminal-side helix, and therefore the helix conformation is not formed. It should be noted that the addition of only two residues (IF) to the C-terminal helix induces Ca^{2+} affinity of peptide IV, since these two side chains probably contribute to hydrophobic contact that stabilises the C-terminal helix.

Concluding remarks

FTIR spectroscopy is a powerful tool for identifying the coordination structures of M^{2+} in Ca^{2+}-binding proteins—that is, the coordination structure modes of side-chain COO^- groups. The downshift of the COO^- antisymmetric stretching mode from 1565 cm^{-1} to 1555–1540 cm^{-1} upon Ca^{2+} binding is a commonly observed feature of FTIR spectra for EF-hand proteins. Apart from the proteins described here, FTIR spectroscopy has already been successfully applied to other EF-hand proteins: recoverin [78], calcineurin B [79], and other Ca^{2+}-binding proteins [23,80,81] that do not belong to EF-hand proteins. FTIR spectroscopy in combination with site-directed mutagenesis will make it possible to more clearly identify the specific amino-acid residues involved in the structure–function correlations of the proteins.

Acknowledgments

This work was supported by the 21st Century Center of Excellence Program and by Grants-in-Aid for Scientific Research from the Ministry of Education, Science, Sports, and Culture of Japan.

References

[1] M.J. Berridge, The interaction of cyclic nucleotides and calcium in the control of cellular activity, Adv. Cyclic Nucleotide Res. 6 (1975) 1–98.
[2] R.H. Kretsinger, in: R.H. Wasserman (Ed.), Calcium Binding Proteins and Calcium Function, Elsevier/Holland, New York, 1977, pp. 63–72.
[3] H.J. Vogel, Calmodulin-a versatile calcium medicated protein, Biochem. Cell. Biol. 72 (1994) 357–376.
[4] I. Niki, H. Yokokura, H. Sudo, M. Kato, H. Hidaka, Ca^{2+} signaling and intracellular Ca^{2+} binding proteins, J. Biochem. 120 (1996) 685–698.
[5] N.S. Poonia, A.V. Bajaj, Coordination chemistry of alkali and alkaline earth cations, Chem. Rev. 79 (1979) 389–445.
[6] J.-P. Declercq, B. Tinant, J. Parello, J. Rambaud, Ionic interactions with parvalbumins. Crystal structure determination of pike 4.10 parvalbumin in four different ionic environments, J. Mol. Biol. 220 (1991) 1017–1039.
[7] A. Houdesse, C. Cohen, Structure of the regulatory domain of scallop myosin at 2 Å resolution: implications for regulation, Structure 4 (1996) 21–32.
[8] G.B. Deacon, R.J. Phillips, Relationships between the carbon–oxygen stretching frequencies of carboxylato complexes and the type of carboxylate coordination, Coord. Chem. Rev. 33 (1980) 227–250.
[9] K. Nakamoto, in: Infrared and Raman Spectra of Inorganic and Coordination Compounds Part B, fifth ed., Wiley, New York, 1997, pp. 57–62.
[10] J.E. Tackett, FT-IR characterization of metal acetates in aqueous-solution, Appl. Spectrosc. (1989) 483–499.
[11] M. Nara, H. Torii, M. Tasumi, Correlation between the vibrational frequencies of the carboxylate group and the types of its coordination to a metal ion: an ab initio molecular orbital study, J. Phys. Chem. (1996) 19812–19817.
[12] H.H. Mantsch, H.L. Casel, D.M. Moffat, in: R.J.H. Clark, R.E. Hester (Eds.), Spectroscopy of Biological Systems, Wiley, Chichester, 1986, pp. 1–46,.
[13] J.L.R. Arrondo, A. Muga, J. Castresana, F.M. Goi, Quantitative studies of the structure of proteins in solution by Fourier-transform infrared spectroscopy, Prog. Biophys. Mol. Biol. 59 (1991) 23–56.
[14] D.M. Byler, H. Susi, Examination of the secondary structure of proteins by deconvolved FTIR spectra, Biopolymers 25 (1986) 469–487.
[15] W.K. Surewicz, H.H. Mantsch, New insight into protein secondary structure from resolution-enhanced infrared-spectra, Biochim. Biophys. Acta 952 (1988) 115–130.
[16] M. Jackson, P.I. Haris, D. Chapman, Fourier-transform infrared spectroscopic studies of lipids, polypeptides and proteins, J. Mol. Struct. 214 (1989) 329–355.
[17] W.K. Surewicz, H.H. Mantsch, D. Chapman, Determination of protein secondary structure by Fourier-transform infrared-spectroscopy. A critical assessment, Biochemistry 32 (1993) 389–394.
[18] J.K. Kauppinen, D.J. Moffatt, H.H. Mantsch, D.G. Cameron, Fourier self-deconvolution- a method for resolving intrinsically overlapped bands, Appl. Spectrosc. 35 (1981) 271–276.
[19] J.K. Kauppinen, D.J. Moffatt, H.H. Mantsch, D.G. Cameron, Fourier-transforms in the computation of self-deconvoluted and 1st–order derivative spectra of overlapped band contours, Anal. Chem. 53 (1981) 1454–1457.
[20] R.N. Jones, K. Shimokoshi, Some observations of the resolution enhancement of spectral data by the method of self-deconvolution, Appl. Spectrosc. 37 (1983) 59–67.
[21] A. Barth, The infrared absorption of amino acid side chains, Prog. Biophys. Mol. Biol. 74 (2000) 141–173.
[22] A. Barth, C. Zscherp, What vibrations tell us about proteins, Q. Rev. Biophys. 35 (2002) 369–430.
[23] M. Mizuguchi, M. Nara, K. Kawano, K. Nitta, FTIR study of the Ca^{2+}-binding to bovine α-lactalbumin. Relationships between the type of coordination and characteristics of the bands due to the Asp COO^- groups in the Ca^{2+}-binding site, FEBS Lett. 417 (1997) 153–157.
[24] M. Nara, M. Tasumi, M. Tanokura, T. Hiraoki, M. Yazawa, A. Tsutsumi, Infrared studies of interaction between metal ions and Ca^{2+}-binding proteins. Marker bands for identifying the types of coordination of the side-chain COO^- groups to metal ions in pike parvalbumin ($pI = 4.10$), FEBS Lett. 349 (1994) 84–88.
[25] M. Nara, M. Tanokura, T. Yamamoto, M. Tasumi, A comparative studies of the binding effects of Mg^{2+}, Ca^{2+}, Sr^{2+}, and Cd^{2+} on calmodulin by Fourier-transform infrared spectroscopy, Biospectroscopy 1 (1995) 47–54.
[26] F. Yumoto, M. Nara, H. Kagi, W. Iwasaki, T. Ojima, K. Nishita, K. Nagata, M. Tanokura, Coordination structures of Ca^{2+} and Mg^{2+} in Akazara scallop troponin C in solution. FTIR spectroscopy of side-chain COO^- groups, Eur. J. Biochem. 268 (2001) 6284–6290.
[27] M. Nara, F. Yomoto, K. Nagata, M. Tanokura, H. Kagi, T. Ojima, K. Nishita, Fourier transform infrared spectroscopic study on the binding of Mg^{2+} to a mutant Akazara scallop troponin C (E142Q), Biopolymers 74 (2004) 77–81.
[28] M. Nara, F. Yomoto, K. Nagata, M. Tanokura, H. Kagi, T. Ojima, K. Nishita, Infrared spectroscopic study on Ca^{2+} binding to Akazara scallop troponin C in comparison with peptide analogues if its Ca^{2+}-binding site IV, Vib. Spectrosc. 42 (2006) 188–191.
[29] M. Nara, H. Morii, F. Yumoto, H. Kagi, M. Tanokura, Fourier transform infrared spectroscopic study on the Ca^{2+}-bound coordination structures of synthetic peptide analogues of the calcium-binding site III of troponin C, Biopolymers 82 (2006) 339–343.
[30] J.F. Pechère, in: R.H. Wasserman, R. Corradino, E. Carafoli, R.H. Kretsinger, D.H. MacLennan, F.L. Siegel (Eds.), Calcium-binding Protein and Calcium, Elsevier, New York, 1977, pp. 213–221.
[31] C.B. Klee, T.H. Crouch, P.G. Richman, Calmolulin, Annu. Rev. Biochem. 49 (1980) 489–515.
[32] C.B. Klee, T.C. Vanaman, Calmodulin, Adv. Protein Chem. 35 (1982) 213–321.
[33] R.H. Kretsinger, C.E. Nockolds, Ionic interactions with parvalbumins. Crystal structure determination of pike 4.10 parvalbumin in four different ionic environments, J. Biol. Chem. 248 (1973) 3313–3326.
[34] P.C. Moews, R.H. Kretsinger, Refinement structure of carp muscle calcium-binding parvalbumin by model-building and difference Fourier-analysis, J. Mol. Biol. 91 (1975) 201–225.
[35] V.D. Kumar, L. Lee, B.F.P. Edwards, Refined crystal-structure of calcium-liganded carp parvalbumin 4.25 at 1.5-Å resolution, Biochemistry 29 (1990) 1404–1412.
[36] P. Lehky, M. Comte, E.H. Fischer, E.A. Stein, New solid-phase chelator with high affinity and selectivity for calcium–parvalbumin–polyacrylamide, Anal. Biochem. 82 (1977) 158–169.
[37] W. Wunk, J.A. Cox, E.A. Stein, in: W.Y. Cheung (Ed.), Calcium and Cell Function, vol. 2, Academic press, New York, 1982, pp. 243–278.
[38] J.P. Declercq, B. Tinant, J. Parello, G. Etienne, R. Huber, Crystal-structure determination and refinement of pike 4.10 parvalbumin (minor component esox-lucius), J. Mol. Biol. 202 (1988) 349–353.
[39] J.A. Cox, Interactive properties of calmodulin, Biochem. J. 249 (1988) 621–629.
[40] Y.S. Babu, J.S. Sack, T.J. Greenhough, C.E. Bugg, A.R. Means, W.J. Cook, Three-dimensional structure of calmodulin, Nature 315 (1985) 37–40.

[41] Y.S. Babu, C.E. Bugg, W.J. Cook, Structure of calmodulin refined at 2.2 Å resolution, J. Mol. Biol. 204 (1988) 191–204.
[42] J.F. Maune, C.B. Klee, K. Beckingham, Ca^{2+}-binding and conformational change in two series of point mutations to the individual Ca^{2+}-binding sites of calmodulin, J. Biol. Chem. 267 (1992) 5286–5295.
[43] Y. Waltersson, S. Linse, P. Brodin, T. Grundstrom, Mutational effects on the cooperativity of Ca^{2+}-binding in calmodulin, Biochemistry 32 (1993) 7866–7871.
[44] D.J. Wolff, P.G. Poireir, C.O. Brostrom, M.A. Brostrom, Divalent cation binding properties of bovine brain Ca^{2+}-dependent regulator protein, J. Biol. Chem. 252 (1977) 4108–4117.
[45] S. Chao, Y. Suzuki, J.R. Zysk, W.Y. Cheung, Activation of calmodulin by various metal cation as a function of ionic radius, Mol. Pharmacol. 26 (1984) 75–82.
[46] D. Rainteau, C. Wolf, F. Lavialle, Effects of calcium and calcium analogues of calmodulin: a Fourier transform infrared and electron spin resonance investigation, Biochem. Biophys. Acta 1011 (1989) 81–87.
[47] J. Haiech, C.B. Klee, abd G. Demaille, Effects of cations on affinity of calmodulin for calcium: ordered binding of calcium ions allows the specific activation of calmodulin-stimulated enzymes, Biochemistry 20 (1981) 3890–3897.
[48] J.R. Dedman, J.D. Potter, R.L. Jackson, J.D. Johnson, A.R. Means, Physicochemical properties of rat testis Ca^{2+}-dependent regulator protein of cyclic nucleotide phosphodiesterase, J. Biol. Chem. 25 (1977) 8415–8422.
[49] K.B. Seamon, Calcium and magnesium-dependent conformational states of calmodulin as determined by nuclear magnetic resonance, Biochemistry 19 (1980) 207–215.
[50] J. Trewhella, W.K. Liddle, D.B. Heidorn, N. Strynadka, Calmodulin and troponin C structures studied by Fourier transform infrared spectroscopy: effects of Ca^{2+} and Mg^{2+} binding, Biochemistry 28 (1989) 1294–1301.
[51] M. Jackson, P.I. Haris, D. Chapman, Fourier-transform infrared spectroscopic studies of Ca^{2+}-binding proteins, Biochemistry 30 (1991) 9681–9686.
[52] M. Zhang, H. Fabian, H.H. Mantsch, H.J. Vogel, Isotope-edited Fourier transform infrared spectroscopy studies of calmodulin's interaction with its target peptides, Biochemistry 33 (1994) 10883–10888.
[53] A.A. Pandyra, A.P. Yamnick, V.V. Andrushchenko, H. Wieser, H.J. Vogel, Isotope-labeled vibrational circular dichroism studies of calmodulin and its interactions with ligands, Biopolymers 79 (2005) 231–237.
[54] S. Ebashi, M. Endo, I. Ohtsuki, in: E. Carafoli, C.B. Klee (Eds.), Calcium as a Cellular Regulator, Oxford Univ. Press, New York, 1999, pp. 579–595.
[55] A.S. Zot, J.D. Potter, Structural aspects of troponin–tropomyosin regulation of skeletal muscle contraction, Ann. Rev. Biophys. Chem. 16 (1987) 535–539.
[56] J.H. Collins, J.D. Potter, M.J. Horn, G. Wilshire, N. Jackman, The amino acid sequence of rabbit skeletal muscle troponin C: gene replication and homology with calcium-binding proteins from carp and hake muscle, FEBS Lett. 36 (1973) 268–272.
[57] J.M. Wilkinson, Troponin C from rabbit slow skeletal and cardiac muscle is the product of a single gene, Eur. J. Biochem. 103 (1980) 179–188.
[58] J.P. van Eerd, K. Takahashi, Determination of the complete amino acid sequence of bovine cardiac troponin C, Biochemistry 15 (1976) 1171–1180.
[59] J.D. Potter, J. Gergely, The calcium and magnesium binding sites on troponin and their role in the regulation of myofibrillar adenosine triphosphatase, J. Biol. Chem. 250 (1975) 4628–4633.
[60] Y. Ogawa, Calcium binding to troponin C and troponin: effects of Mg^{2+}, ionic strength and pH, J. Biochem. 97 (1985) 1011–1023.
[61] S. Morimoto, The effect of Mg^{2+} on the Ca^{2+} binding to troponin C in rabbit fast skeletal myofibrils, Biochim. Biophys. Acta 1073 (1991) 336–340.
[62] S. Linse, S. Forsén, in: A.R. Means (Ed.), Calcium Regulation of Cellular Function, vol. 30, Raven Press, New York, 1995, pp. 89–152.
[63] J. Evenäs, A. Malmendal, S. Forsén, Calcium, Curr. Opin. Chem. Biol. 2 (1998) 293–302.
[64] W. Lehman, J.F. Head, P.W. Grant, The stoichiometry and location of troponin I- and troponin C-like proteins in the myofibril of the bay scallop, Aequipecten irradians, Biochem. J. 171 (1980) 413–418.
[65] T. Ojima, K. Nishita, Troponin from Akazara scallop striated adductor muscles, J. Biol. Chem. 261 (1986) 16749–16754.
[66] T. Ojima, K. Nishita, Akazara scallop troponin C: Ca^{2+}-induced conformational change and interaction with rabbit troponin subunits, Arch. Biochem. Biophys. 299 (1992) 344–349.
[67] O. Herzberg, M.N. G James, Structure of the calcium regulatory muscle protein troponin-C at 2.8 Å resolution, Nature 313 (1985) 653–659.
[68] K.A. Satyshur, S.T. Rao, D. Pyzalska, W. Drendel, M. Greaser, M. Sundarlingam, Refined structure of chicken skeletal muscle troponin C in the two-calcium state at 2 Å resolution, J. Biol. Chem. 263 (1988) 16620–16628.
[69] S.W. Provencher, J. Glöckner, Estimation of globular protein secondary structure from circular dichroism, Biochemistry 20 (1981) 33–37.
[70] A. Malmendal, J. Evenäs, E. Thulin, G.P. Gippert, T. Drakenberg, S. Forsén, When size is important. Accommodation of magnesium in a calcium binding regulatory domain, J. Biol. Chem. 273 (1998) 28994–29001.
[71] T. Ojima, N. Koizumi, K. Ueyama, A. Inoue, K. Nishita, Functional role of Ca^{2+}-binding site IV of scallop troponin C, J. Biochem. 128 (2000) 803–809.
[72] R.E. Reid, J. Gariepy, A.K. Saund, R.S. Hodges, Calcium-induced protein folding, J. Biol. Chem. 256 (1981) 2742–2751.
[73] B.J. Marsden, R.S. Hodges, B.D. Sykes, A ^1H NMR determination of the solution conformation of a synthetic peptide analogue of calcium-binding site III of rabbit skeletal troponin C, Biochemistry 28 (1989) 8839–8847.
[74] G.S. Shaw, R.S. Hodges, B.D. Sykes, Probing the relationship between a-helix formation and calcium affinity in troponin C: ^1H NMR studies of calcium binding to synthetic and variant site III helix-loop-helix peptides, Biochemistry 30 (1991) 8339–8347.
[75] G.S. Shaw, in: H.J. Hans (Ed.), Methods in Molecular Biology, vol. 173, Humana, Totowa, NJ, 2001, pp. 175–181.
[76] T. Ojima, M. Maita, A. Inoue, K. Nishita, Bacterial expression, purification, and characterization of akazara scallop troponin C, Fish. Sci. 63 (1997) 137–141.
[77] A. Houdusse, M.L. Love, R. Dominguez, Z. Grabarek, C. Cohen, Structures of four Ca^{2+}-bound troponin C at 2.0 angstrom resolution: further insights into the Ca2+-switch in the calmodulin superfamily, Structure 5 (1997) 1695–1711.
[78] T. Ozawa, M. Fukuda, M. Nara, A. Nakamura, Y. Komine, K. Kohama, Y. Umezawa, How can Ca^{2+} selectively activate recoverin in the presence of Mg^{2+}? Surface plasmon resonance and FT-IR spectroscopic studies, Biochemistry 39 (2000) 14495–14503.
[79] S.C. Gallagher, Z.-H. Gao, S. Li, R.B. Dyer, J. Trewhella, C.B. Klee, There is communication between all four Ca^{2+}-bindings sites of calcineurin B, Biochemistry 40 (2001) 12094–12102.
[80] M. Mizuguchi, M. Nara, Y. Ke, K. Kawano, T. Hiraoki, K. Nitta, Fourier-transform infrared spectroscopic studies on the coordination of the side-chain COO^- groups to Ca^{2+} in quine lysozyme, Eur. J. Biochem. 250 (1997) 72–76.
[81] M. Mizuguchi, R. Fujisawa, M. Nara, K. Nitta, K. Kawano, Fourier-transform infrared spectroscopic study of Ca^{2+}-binding to osteocalcin, Cal. Tissue Int. 69 (2001) 337–342.